Iron Abundance Profiles of 12 Clusters of Galaxies Observed With BeppoSAX

Jimmy A. Irwin – University of Michigan
Joel N. Bregman – University of Michigan

Citation of published version:

Irwin, J., Bregman, J. (2001): Iron Abundance Profiles of 12 Clusters of Galaxies Observed With BeppoSAX. *The Astrophysical Journal*, 546(1). DOI: 10.1086/318240

THE ASTROPHYSICAL JOURNAL, 546:150–156, 2001 January 1

IRON ABUNDANCE PROFILES OF 12 CLUSTERS OF GALAXIES OBSERVED WITH *BeppoSAX*

JIMMY A. IRWIN[1] AND JOEL N. BREGMAN
Department of Astronomy, University of Michigan, Ann Arbor, MI 48109-1090; jirwin@astro.lsa.umich.edu, jbregman@umich.edu
Received 2000 March 27; accepted 2000 September 5

ABSTRACT

We have derived azimuthally averaged radial iron-abundance profiles of the X-ray gas contained within 12 clusters of galaxies with redshift $0.03 \leq z \leq 0.2$ observed with *BeppoSAX*. We find evidence for a negative metal-abundance gradient in most of the clusters, particularly significant in clusters that possess cooling flows. The composite profile from the 12 clusters resembles that of cluster simulations of Metzler & Evrard. This abundance gradient could be the result of the spatial distribution of gas-losing galaxies within the cluster being more centrally condensed than the primordial hot gas. Both inside and outside the core region we find a higher abundance in cooling-flow clusters than in non–cooling-flow clusters. Outside of the cooling region this difference cannot be the result of more efficient sputtering of metals into the gaseous phase in cooling-flow clusters but might be the result of the mixing of low-metallicity gas from the outer regions of the cluster during a merger.

Subject headings: cooling flows — galaxies: clusters: general — intergalactic medium — X-rays: galaxies

1. INTRODUCTION

The presence of metals in the hot gas contained within clusters of galaxies provides important clues as to how metals are deposited into the intracluster medium (ICM) from the constituent galaxies of the cluster. The two most likely mechanisms for injecting metals into the ICM are through ram pressure stripping of the gas from galaxies by the ICM (e.g., Gunn & Gott 1972; Gaetz, Salpeter, & Shaviv 1987) and galactic winds (e.g., Ostriker & Yahil 1973; Metzler & Evrard 1994). Recent work has suggested that negative radial-abundance gradients are a common feature in clusters. Analysis of *ASCA* data has indicated that in some clusters the metal abundance declines from $\sim$40%–60% of solar in the center to $\sim$20% of solar at a distance of 0.5–1 Mpc (Ezawa et al. 1997; Ikebe et al. 1997; Sarazin, Wise, & Markevitch 1998; Finoguenov, David, & Ponman 2000; Dupke & White 2000a, 2000b).

Most of the above studies, however, dealt with groups or cooler clusters. The large, energy-dependent point-spread function (PSF) of *ASCA* preferentially scatters hard photons, making spatially resolved spectroscopy problematic for hot clusters. Whereas the problem is less severe for cooler (<5 keV) clusters, substantial errors in the radial temperature and abundance profiles can occur if the PSF is not dealt with properly (see Takahashi et al. 1995). As such, little observational work has been done on the radial-abundance profiles of hotter clusters. There has also been correspondingly little theoretical work performed on the predicted abundance profiles of clusters from hydrodynamical simulations. White (2000) has derived PSF-corrected abundance profiles for a large sample of clusters observed with *ASCA*, but the deconvolution technique used to correct for the PSF unfortunately led to rather large uncertainties in the derived abundance profiles. As a result, only weak constraints could be placed on the presence of abundance gradients from these data.

BeppoSAX is better suited to perform spatially resolved spectroscopy on hot clusters. The PSF of *BeppoSAX* is one-half that of the *ASCA* Gas Imaging Spectrometer and, more importantly, is only weakly dependent on energy. The abundance profiles of five higher temperature clusters have already been derived from *BeppoSAX*, finding at least marginal evidence for abundance gradients in A2029, A2256, A3266, and PKS 0745−191, with no evidence for a gradient in A2319 (De Grandi & Molendi 1999a, 1999b; Molendi et al. 1999; Molendi & De Grandi 1999; Molendi, De Grandi, & Fusco-Femiano 2000). In this paper we increase this sample size by analyzing *BeppoSAX* archival data for 12 clusters of galaxies and derive radial-abundance profiles for each cluster, nine of which have temperatures greater than 5 keV. Throughout this paper we assume $H_0 = 50$ km s^{-1} Mpc^{-1} and $q_0 = 0.5$.

2. SAMPLE AND DATA REDUCTION

From the *BeppoSAX* Science Data Center (SDC) archive,[2] we have obtained data for 12 clusters of galaxies. Within this sample, eight of them possess cooling flows (A85, A496, A1795, A2029, A2142, A2199, A3562, and 2A 0335+096), and four do not (A2163, A2256, A2319, and A3266). We define a cluster as having a cooling flow if the cooling rate is greater than 20 $M_\odot$ yr^{-1} (see White, Jones, & Forman 1997; Peres et al. 1998). All of the clusters are at low redshift ($0.03 \leq z \leq 0.09$) except for A2163, which has a redshift of $z = 0.203$. We analyze data taken with the Medium Energy Concentrator Spectrometer (MECS) on board *BeppoSAX*. The MECS (see Boella et al. 1997 for details) is composed of two identical gas scintillation proportional counters (three detectors before 1997 May 9) that are sensitive in the 1.3–10.5 keV energy range. The event files for all 12 clusters were subjected to the standard screening criteria of the *BeppoSAX* SDC.

Since we are interested in deriving the radial-abundance profiles for these clusters, it is important to account for scattering owing to the PSF of the MECS instrument. Fortunately, the detector+telescope PSF of *BeppoSAX* is nearly independent of energy. This is because the Gaussian PSF of the MECS detector improves with increasing energy, while the PSF of the grazing incidence mirror unit degrades with increasing energy (D'Acri, De Grandi, &

[1] Chandra Fellow.

[2] The SDC archive is available at http://www.sdc.asi.it/sax_main.html.

Molendi 1998), leading to a partial cancellation when these two effects are combined.

To correct for the PSF, we have used the routine EFFAREA, available as part of the SAXDAS 2.0 suite of *BeppoSAX* data reduction programs. The program EFFAREA convolves the surface-brightness profile of the cluster (which has been determined using *ROSAT* PSPC data; see Ettori & Fabian 1999; Mohr, Mathiesen, & Evrard 1999) with the PSF of the MECS to determine the amount of contamination in the spatial region in question at each energy from other regions of the cluster. Thus, an energy-dependent correction vector is formed. When this correction vector is multiplied by the observed spectrum, the PSF-corrected energy spectrum is obtained for the region. In practice, this information is incorporated into the auxiliary response file (the .arf file), which is subsequently used in the spectral fitting. This task also corrects for vignetting. A more complete description of the task is given in Molendi (1998)[3] and D'Acri et al. (1998). This correction does not appear to affect the spectrum greatly; D'Acri et al. (1998) and Kaastra, Bleeker, & Mewe (1998) found only small changes between the uncorrected and corrected temperature profiles for Virgo and A2199, respectively. In addition, D'Acri et al. (1998) found that the correction vectors amounted to 5% or less for energies above 3 keV outside of the innermost bin (the innermost bin loses some flux via scattering but gains very little from photons scattered in from greater off-axis radii). Our inner three spatial bins are identical in angular extent to the bins of D'Acri et al. (1998), so we assume that our correction vectors are as small as theirs. In addition, we find only a small difference between our corrected and uncorrected abundance profiles for our sample.

We extracted spectra in four annular regions for each cluster, with inner and outer radii of 0′–2′, 2′–4′, 4′–6′, and 6′–9′. At 9′ the telescope entrance-window support structure (the strongback) strongly absorbs X-rays, making spectroscopy difficult in this area of the detector. In addition, for off-axis angles greater than 10′, the departure of the PSF from radial symmetry becomes noticeable (Boella et al. 1997). With this in mind, we ended the radial profiles at 9′. At this radius, the profiles extended to 17%–33% of the virial radius, where $r_{\rm virial} = 3.9(T/10\ {\rm keV})^{1/2}$ Mpc (see Evrard, Metzler, & Navarro 1996) for all clusters except A2163, for which the profile extended to 55% of $r_{\rm virial}$. We also extracted one global spectrum (0′–9′) and also two spectra covering the two regions 0–$0.075r_{\rm virial}$ and 0.075–$0.173r_{\rm virial}$. Background was obtained from the deep blank sky data provided by the SDC. We used the same region filter to extract the background as we did the data, so that both background and data were affected by the detector response in the same manner. The energy channels were regrouped to contain at least 25 counts.

For each cluster, XSPEC Version 11.0 was used to fit the spectrum. The MECS2 and MECS3 (and MECS1 when available) data were fitted separately but with the same temperature, metallicity, and normalization. We assumed a MEKAL model with an absorption component fixed at the Galactic value, allowing the temperature and metallicity to vary. For the iron-to-hydrogen ratio, we use a value of 4.68×10^{-5} (Anders & Grevesse 1989) since this is the value assumed for most previous abundance determinations, although it should be noted that more recent determinations of the Fe/H ratio point to a value of 3.24×10^{-5} (Ishimaru & Arimoto 1997). Because of a systematic shift of 45–50 eV at 6.6 keV in the MECS channel–to–energy conversion, we have also allowed the redshift to vary (F. Fiore 1999, private communication). This systematic shift was evident in our sample; when the redshift was allowed to vary, the measured redshift was less than the optically determined redshift in all 12 clusters and inconsistent with the optically determined redshift at the 90% confidence level for eight of them. A modest decrease in the reduced χ^2 also occurred for most of the clusters when the redshift was allowed to vary. However, freeing the redshift did not affect the values obtained for the temperature and metallicity by more than 5% (and in most instances much less), so the results do not depend significantly on this shift. We also fitted only the 3.0–10.5 keV part of the spectrum because of excess flux found below 3.0 keV that might be the result of uncertainties in the calibration of the MECS instruments; see Irwin & Bregman (2000) for a more complete description. All quoted errors are 90% confidence levels for one interesting parameter ($\Delta\chi^2 = 2.71$) unless otherwise noted. Below we present the results from the abundance analysis. The results of the temperature analysis are given in Irwin & Bregman (2000). One additional cluster (A3562) not analyzed in Irwin & Bregman (2000) is presented here.

3. ABUNDANCE OF THE HOT GAS

3.1. *Global Abundances*

For hot clusters, it is the Fe Kα line that primarily determines the metal-abundance measurement. The fits to the global spectra were adequate, with $\chi^2_\nu < 1.20$ in all cases. For the eight clusters harboring cooling flows, the weighted average emission-weighted global abundance was 0.37 ± 0.04 (the error is given by the weighted standard deviation for the subsample). The four clusters lacking cooling flows had an average emission-weighted global abundance of 0.27 ± 0.02. The ratio of cooling-flow to noncooling-flow global abundance is 1.4 ± 0.2, in good agreement with the value of 1.6 obtained by Allen & Fabian (1998) with a sample of 30 clusters observed with *ASCA* when they used a single-component thermal model.

3.2. *Radial-Abundance Profiles*

The radial metal-abundance profile for each cluster is shown in Figure 1. Four of the clusters have had abundance gradients determined with *ASCA* and are generally consistent within the errors with the profiles determined here: A496 (Finoguenov et al. 2000; Dupke & White 2000b), A2199 (Finoguenov et al. 2000), A2029 (Sarazin et al. 1998; Finoguenov et al. 2000), and 2A 0335+096 (Kikuchi et al. 1999). In addition, analysis of this same *BeppoSAX* data for A2029, A2256, A2319, and A3266 by other authors is in agreement with our results (De Grandi & Molendi 1999b; Molendi & De Grandi 1999; Molendi et al. 1999), with the exception of A2256 for which Molendi et al. (2000) found a significantly decreasing profile, whereas ours is flat. However, our inability to find an abundance gradient is the result of the short observing time of the data we used; the total observing time of the Molendi et al. (2000) observation was 2.6 times longer than ours, and they were able to place much tighter constraints on the abundance than we were. In both studies, the 1 σ error bars overlapped one another.

[3] The Molendi 1998 *BeppoSax* Technical Report can be found at ftp://www.sdc.asi.it/pub/sax/doc/reports.arf_extended_sources.ps.gz.

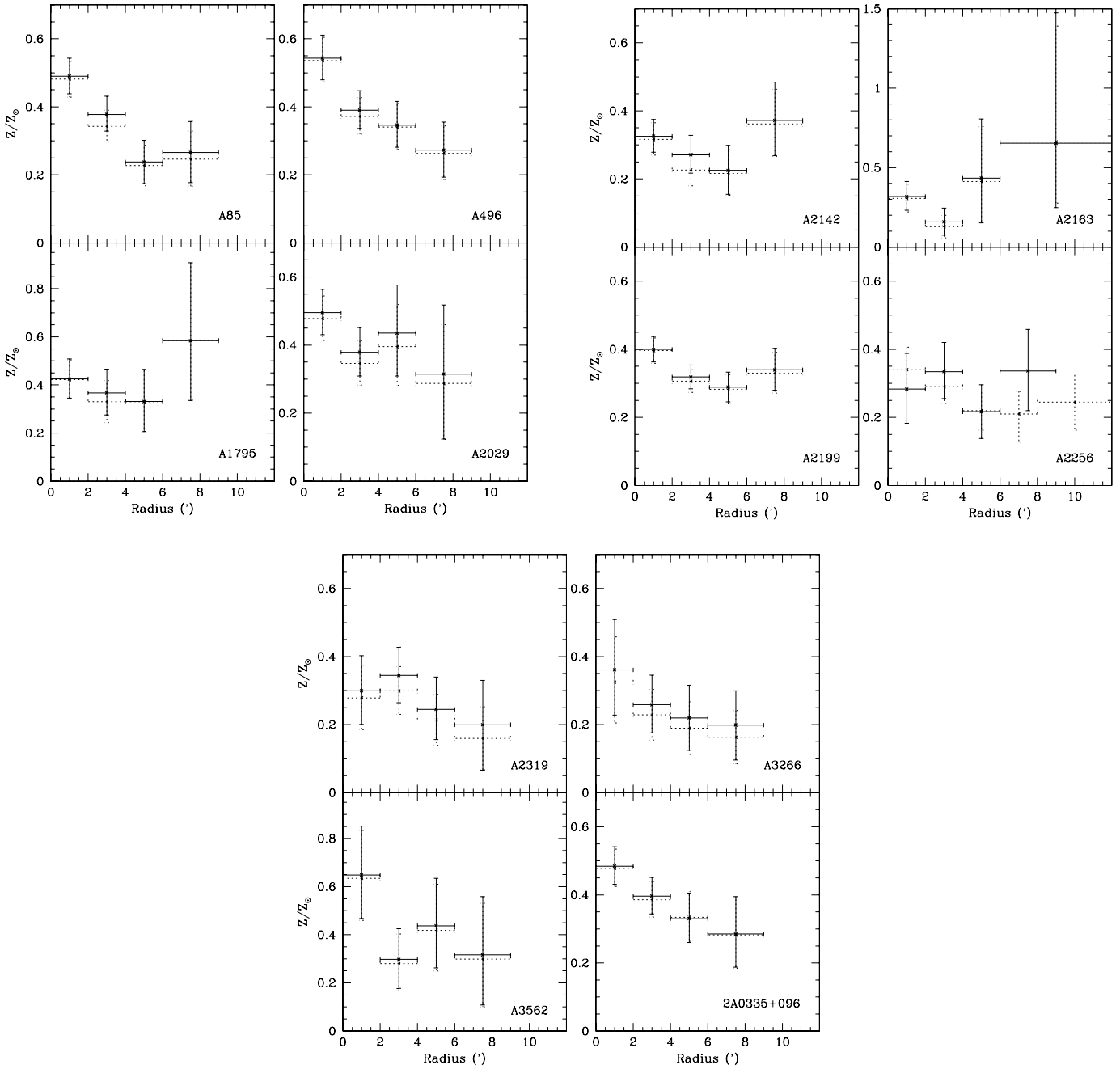

FIG. 1.—Radial-abundance profiles for the 12 clusters in the sample with 90% confidence levels, derived from spectral fitting in the 3.0–10.5 keV energy range. Solid lines represent abundances corrected for the PSF of *BeppoSAX*, and dotted lines are uncorrected for the PSF, except for A2256 where the dotted line represents the *BeppoSAX* profile derived by Molendi et al. (2000) from a longer observation (their error bars have been multiplied by 1.65 to convert 68% confidence levels to 90% confidence levels).

In general, the abundance profiles decline with radius. Such a trend was also found in clusters observed by *ASCA* (Finoguenov et al. 2000; Kikuchi et al. 1999; Dupke & White 2000a), although there are notable exceptions to this trend such as A1060 (Tamura et al. 1996). These previous studies focused primarily on cooler clusters ($kT < 5$ keV). This study confirms the ubiquity of negative abundance gradients in hotter clusters (nine of our 12 clusters have $kT > 5$ keV), as illustrated in Figure 2, where all 12 abundance profiles, normalized to the global abundance for each cluster, are plotted versus radius in units of the virial radius. A strong negative gradient in the abundance profile is evident out to 25% of the virial radius. However, there are a few points quite discordant with this trend at large radii. The clusters responsible for these discordant points are A1795, A2142, and A2163.

We investigated the possibility that the use of single-component temperature models in the central regions of cooling-flow clusters has biased the determination of the abundance in these regions. The addition of a cooling-flow component did not lead to a significant improvement in the fits, and the cooling rate was only weakly constrained. This is a result of excluding data below 3.0 keV, where the effect of cooling flows on the spectra is most pronounced. When we fixed the cooling rate at values determined by other satellites, the best-fit abundance value was actually slightly

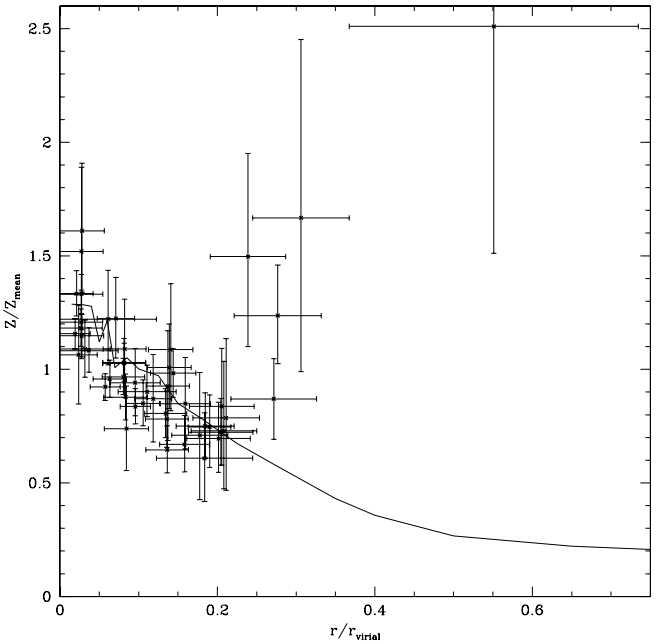

FIG. 2.—Normalized abundance profiles for all 12 clusters in the sample vs. radius in units of the virial radius. Here, the error bars represent the 1 σ errors. A significant radial gradient in the abundance is evident. The solid line represents the composite abundance profile of 18 realizations of the cluster simulations of Metzler & Evrard (1997).

higher than in the single-component case by a few percent, indicating that the central enhancement in the abundance is real.

We have fitted a linear model of the form $(Z/Z_{\rm mean}) = a - b(r/r_{\rm virial})$ to the data. While including all values, the fit is not very good, with $\chi^2 = 72.2$ for 47 degrees of freedom (dof), and can be excluded at greater than 98% confidence level. Removal of the four discordant data points yielded an excellent fit, with $\chi^2 = 46.1$ for 43 dof for values of $a = 1.212$ and $b = 2.705$ (2.149–3.250 at 90% confidence). Although it is not clear why four of the clusters show a $\sim 2\ \sigma$ departure from the observed trend outside $\sim 25\%$ of the virial radius, the derived slope is nonetheless an accurate representation of the data inside of 25% of the virial radius. Excluding non–cooling-flow clusters in addition to the discordant points led to the same best-fit slope.

3.3. *Comparison to Theoretical Models*

Surprisingly little theoretical work has been performed to date to quantify the behavior of abundance gradients in clusters. One such study is that of Metzler & Evrard (1997), who used gasdynamical simulations that included the effects of galactic winds to generate an ensemble of 18 realizations of clusters spanning a wide range of temperatures. Assuming that the iron present in the gas resulted from the ejection of metals from galaxies, a composite iron-abundance profile for the 18 realizations was determined. It was found to decrease significantly with increasing radius. This resulted from the spatial distribution of the galaxies being more centrally condensed than the original primordial X-ray gas. Since the ejected gas traces the galaxies, an abundance gradient is created relative to the primordial gas.

The composite iron-abundance profile from the 18 three-dimensional realizations of Metzler & Evrard (1997) is shown superposed on the *BeppoSAX* data in Figure 2 as a solid line. The composite profile was normalized assuming an average global abundance of 40% of the solar value. Metzler & Evrard (1997) scaled each cluster in radial units of r_{170} before merging the profiles, where r_{170} is the radius within which the mean density is 170 times the critical density. This is very close to our adopted value of $r_{\rm virial}$. The normalized abundance profile of Metzler & Evrard (1997) matches the data very well, ranging from a value of 1.3 in the center to about 0.6 at 25% of the virial radius.

We note that recent work by Finoguenov et al. (2000) and Dupke & White (2000b) has shown that significant radial gradients exist in the elemental abundance ratios in clusters. This would argue against the idea that a difference in the spatial distribution between the galaxies and the gas is responsible for the observed abundance gradient if it is assumed that both Type Ia and Type II elements were released into the ICM under the same conditions. The observational evidence implies that Type Ia and Type II elemental contamination is not the same in the inner and outer parts, with Type Ia ejecta being dominant in the center. Dupke & White (2000b) propose that the observed abundance ratios can be explained by a phase of early, vigorous protogalactic wind driven by Type II supernovae that spread metals uniformly throughout the cluster, followed by a phase of less vigorous Type Ia supernovae wind that was suppressed by the central dominant galaxy in the center of the cluster. Thus, the measured iron abundances originate from a combination of Type II supernovae (having no radial gradient) and Type Ia supernovae (having a radial gradient). The gradient we measure is the linear combination of these two effects.

3.4. *Cooling- versus Non–Cooling-flow clusters*

Inspection of the abundance profiles of the eight cooling-flow clusters reveals a radially decreasing trend in all of them. The gradient is quite significant in A85, A496, A2199, A3562, and 2A 0335+096 and less significant in A1795, A2029, and A2142. This seems to be a universal trend in cooling-flow clusters since all nine cooling-flow clusters in the sample of Finoguenov et al. (2000), as well as all three clusters in the samples of Kikuchi et al. (1999) and Dupke & White (2000a), show the same trend, at least marginally. No clear trend exists among the non–cooling-flow clusters. The profile of A2256 is flat, although a decline with radius cannot be ruled out owing to the large errors (a decline was seen with a longer *BeppoSAX* observation by Molendi et al. 2000; see Fig. 1). A2319, A3266, and A2163 show some evidence for a negative gradient, although the profiles are formally consistent with a flat profile. Results with *ASCA* for clusters with little or no cooling flows are also mixed. Whereas Coma, A401, A1060, and A2670 show a flat abundance profile, A399 has an abundance gradient (Fujita et al. 1996; Tamura et al. 1996; Watanabe et al. 1997; Finoguenov et al. 2000). It is possible that mergers that could be responsible for the disruption of the cooling flow in clusters can also destroy abundance gradients. The degree to which the abundance gradient remains intact may be an indicator of how recent and/or violent the merger was. All four non–cooling-flow clusters are merger candidates. Of the five cooling-flow clusters with significant gradients, only A85 is a merger candidate. Of the three cooling-flow clusters with only weak evidence for an abundance gradients, two are recent merger candidates. Oegerle & Hill (1994) conclude that the velocity distribution of galaxies within A1795 sug-

gests that the cluster underwent a merger with a relatively small subcluster such that the cooling flow was not disrupted. Oegerle, Hill, & Fitchett (1995) also find evidence for subclustering from the galaxy velocity distribution in A2142. *ROSAT* PSPC and HRI images of A2142 also suggest that a merger is in process (Henry & Briel 1996). It is possible that mergers have mixed the gas of these two clusters enough to decrease the significance of an abundance gradient without destroying the cooling flow. A2029 does not show evidence for a merger, although the lack of a significant abundance gradient may be the result of poor photon statistics rather than a lack of a gradient. Further studies of A2029 will be needed to confirm this.

As suggested by Fabian et al. (1994) and Allen & Fabian (1998), the presence of abundance gradients in cooling-flow clusters provides a reasonable explanation as to why cooling-flow clusters have higher emission-weighted metal abundances than their noncooling-flow counterparts. If the cooling gas at the center of clusters has a higher abundance than the outer regions, the strongly peaked X-ray surface-brightness distribution characteristic of cooling-flow clusters will preferentially weight the global emission-weighted abundance toward the central value, with the low-abundance outer regions contributing relatively little to the global value. Such an effect is not present in non–cooling-flow clusters owing to the broader, less-peaked X-ray surface-brightness distribution of these clusters. But is this the only reason for the higher measured metallicity in cooling-flow clusters, or is there really an abundance difference between cooling-flow and non–cooling-flow clusters? To test this, we determined abundances in two regions for each cluster, a circle with a radius of $0.075r_{\rm virial}$ and an annulus with inner and outer radii of $0.075r_{\rm virial}$ and $0.173r_{\rm virial}$. The outer radius was set by the need to extend the annulus no further than 9′ for any cluster, and the inner radius was set to be larger than the cooling radius for any of the cooling-flow clusters.

The results are shown in Table 1. Inside of $0.075r_{\rm virial}$ the cooling-flow subsample had an average abundance of 0.42 ± 0.06, while the noncooling-flow subsample had an average of 0.33 ± 0.04. In the outer region the cooling-flow subsample had an average abundance of 0.30 ± 0.02, while the noncooling-flow subsample had an average of 0.24 ± 0.03. Thus, there appears to be an abundance gradient in non–cooling-flow clusters as well as cooling-flow clusters. The presence of abundance gradients in non–cooling-flow clusters (especially in hot clusters) would seem to rule out claims that previously observed abundance gradients were artifacts of incorrect spectral modeling due to either the presence of cooling gas at the center of clusters or uncertainties in modeling the Fe L line complex for cooler clusters.

Although the average abundances of the cooling-flow and non–cooling-flow clusters are marginally consistent within the errors within the cooling region, the data suggests that there is a discrepancy between the abundance of cooling and non–cooling-flow clusters outside of the cooling radius. Of course, any conclusions drawn from a subsample of four clusters should be viewed with caution. A larger sample of clusters will be necessary to confirm if the abundance differences between cooling-flow and non–cooling-flow clusters are real. This result is in the opposite sense expected if higher metallicity gas from the cooling-flow region has been mixed in with the lower metallicity gas of the outer regions as the result of a merger in a present-day non–cooling-flow cluster. This trend also appeared in a sample of clusters observed by *ASCA*. Fukazawa et al. (1998) analyzed 26 clusters with temperatures of at least 3.0 keV and found global abundances after having excised the inner cooling regions. The average abundance for the 16 cooling-flow clusters was 0.29 ± 0.07, while the average for the ten non–cooling-flow clusters was 0.23 ± 0.05. Although at a lower significance than our *BeppoSAX* sample, the trend is in the same direction. Fukazawa et al. (1998) did not claim to extract their spectra in units of the virial radius, which is the unit of distance that allows the most direct comparison of radial properties for clusters of varying sizes and temperatures. This might wash out some of the information on the abundance gradient when the profiles are combined and lead to a result of lower statistical significance.

Allen & Fabian (1998) present the interesting scenario in which metallicity gradients can be explained (at least in part) by a significant fraction of the metals in clusters residing on grains in cluster cores. Since the lifetime of a grain to sputtering in the hot ICM is inversely proportional

TABLE 1

ABUNDANCES

Cluster	kT[a] (keV)	Global	χ^2_ν/dof	0–$0.075r_{\rm virial}$	0.075–$0.173r_{\rm virial}$
A85[b]	$6.4^{+0.3}_{-0.2}$	$0.37^{+0.03}_{-0.03}$	1.17 / 282	$0.45^{+0.04}_{-0.04}$	$0.30^{+0.04}_{-0.05}$
A496[b]	$4.2^{+0.1}_{-0.1}$	$0.41^{+0.03}_{-0.03}$	1.20 / 259	$0.48^{+0.05}_{-0.04}$	$0.31^{+0.05}_{-0.05}$
A1795[b]	$6.0^{+0.4}_{-0.4}$	$0.39^{+0.05}_{-0.05}$	0.97 / 211	$0.41^{+0.08}_{-0.07}$	$0.36^{+0.09}_{-0.09}$
A2029[b]	$7.6^{+0.5}_{-0.4}$	$0.43^{+0.05}_{-0.04}$	0.98 / 141	$0.49^{+0.06}_{-0.06}$	$0.30^{+0.08}_{-0.07}$
A2142[b]	$8.7^{+0.4}_{-0.4}$	$0.30^{+0.03}_{-0.03}$	1.02 / 292	$0.32^{+0.05}_{-0.05}$	$0.26^{+0.05}_{-0.05}$
A2163	$11.7^{+1.0}_{-0.9}$	$0.26^{+0.06}_{-0.06}$	1.05 / 440	$0.39^{+0.17}_{-0.14}$	$0.21^{+0.07}_{-0.07}$
A2199[b]	$4.4^{+0.1}_{-0.1}$	$0.35^{+0.02}_{-0.02}$	1.03 / 419	$0.37^{+0.03}_{-0.03}$	$0.31^{+0.04}_{-0.03}$
A2256	$7.1^{+0.5}_{-0.4}$	$0.28^{+0.04}_{-0.04}$	1.06 / 238	$0.31^{+0.09}_{-0.08}$	$0.28^{+0.06}_{-0.06}$
A2319	$10.5^{+0.8}_{-0.7}$	$0.28^{+0.05}_{-0.05}$	1.04 / 273	$0.36^{+0.07}_{-0.07}$	$0.22^{+0.06}_{-0.06}$
A3266	$9.9^{+0.8}_{-0.7}$	$0.24^{+0.05}_{-0.05}$	0.93 / 265	$0.28^{+0.10}_{-0.10}$	$0.23^{+0.07}_{-0.06}$
A3562[b]	$5.1^{+0.6}_{-0.5}$	$0.40^{+0.08}_{-0.08}$	0.95 / 165	$0.53^{+0.15}_{-0.14}$	$0.30^{+0.11}_{-0.10}$
2A 0335+096[b]	$3.2^{+0.08}_{-0.08}$	$0.41^{+0.03}_{-0.03}$	1.13 / 257	$0.47^{+0.05}_{-0.05}$	$0.33^{+0.05}_{-0.04}$

[a] Best-fit global temperature of *BeppoSAX* data from Irwin & Bregman 2000, except for A3562, which is presented here for the first time.

[b] Cooling-flow cluster.

to the electron density of the hot gas (e.g., Draine & Salpeter 1979), more metals would be released into the gas phase in the high-density cooling-flow regions of clusters than in lower density regions, providing the dust grains are ≥ 10 μm. By extending this argument outside the core region, it might be possible to explain the difference in metallicity at large radii between cooling-flow and non–cooling-flow clusters. If the density of gas outside the core is greater in cooling-flow clusters than in non–cooling-flow clusters, more metals will be released into the gas phase for the former. A difference in density among cooling and non–cooling-flow clusters outside of 200 kpc was observed by White et al. (1997), who deprojected the surface-brightness profiles of 207 clusters observed with *Einstein Observatory* and found that the electron densities of clusters with cooling rates greater than 10 $M_\odot$ yr^{-1} were larger than for clusters with cooling rates less than 10 $M_\odot$ yr^{-1} out to a radius of 1 Mpc. For a 7 keV cluster, our 0.075–0.173$r_{\rm virial}$ bin corresponds to 240–560 kpc. At a radius of 450 kpc, White et al. (1997) found that the cooling-flow clusters had an electron density of $\sim 7 \times 10^{-4}$ cm^{-3}, whereas the non–cooling-flow clusters had an electron density of $\sim 3 \times 10^{-4}$ cm^{-3}. For a grain lifetime of $(2 \times 10^6)a/n_e$ yr (where a is the size of the grain in microns and n_e is the electron density of the hot gas in cm^{-3}), grains with a size of around 2 μm would survive in non–cooling-flow clusters for a Hubble time while being sputtered in cooling-flow clusters. While rather large, dust grains of this size are not unreasonable. In addition, this argument assumes that the dust was deposited into the ICM at the time the cluster was created. In reality, dust is deposited into the ICM throughout the history of the cluster, allowing smaller dust grains to survive in low-density non–cooling-flow clusters while still being sputtered in high-density cooling-flow clusters. This in turn can lead to a higher abundance in the outer regions of cooling-flow clusters since more of the grains have been sputtered away owing to the higher electron density.

However, more recent determinations of the density profiles of clusters determined with *ROSAT* PSPC data indicate that the non–cooling-flow clusters in our sample do not have a lower electron density in the 0.075–0.173$r_{\rm virial}$ region than the cooling-flow clusters (J. Mohr 2000, private communication). At 10% of the virial radius the average electron density for the non–cooling-flow clusters A2256, A2319, and A3266 was $(1.80 \pm 0.20) \times 10^{-3}$ cm^{-3}, while for the cooling-flow clusters A85, A496, A1795, A2029, A2142, A2199, and A3562 the average electron was $(1.92 \pm 0.46) \times 10^{-3}$ cm^{-3} Thus, it does not appear likely that the difference in abundances outside the cooling radius can be the result of an increased sputtering of grains in cooling-flow clusters.

Since non–cooling-flow clusters are usually merger candidates, one possible explanation for the difference in abundances between cooling and non–cooling-flow clusters is the mixing of gas via mergers from larger ($>0.175r_{\rm virial}$) radii rather than from gas interior to this region. If the iron abundance of the gas continues to decline with increasing radius beyond $0.2r_{\rm virial}$ as the simulations of Metzler & Evrard (1997) imply, the mean metallicity in our 0.075–0.173 $r_{\rm virial}$ bin will be lowered upon mixing with this low-metallicity gas during a merger. A2142, a cooling-flow cluster that is thought to be undergoing a merger and shows only weak evidence for an abundance gradient, also has the lowest metallicity in the 0.075–0.173 $r_{\rm virial}$ bin among cooling-flow clusters in our sample, consistent with the merger-mixing theory. However, A1795, which is also believed to have recently experienced a merger, has a high metallicity value in the 0.075–0.173 $r_{\rm virial}$ bin, although the uncertainty is rather large. A larger sample of clusters with abundances determined out to larger radii will be needed to explore this topic further.

4. CONCLUSIONS

We have analyzed 12 clusters with the MECS instrument on board *BeppoSAX* and find evidence for a negative abundance gradient in most of them. This gradient is present in all eight cooling-flow clusters and to a lesser significance in the non–cooling-flow clusters. Since $kT > 5$ keV for nine of the 12 clusters, this work extends the ubiquity of abundance gradients to hot clusters. The slope of the abundance gradient is in good agreement with cluster simulations performed by Metzler & Evrard (1997). In our sample cooling-flow clusters had a higher metallicity than non–cooling-flow clusters both in the inner regions of the cluster and the outer regions out to several hundred kpc; further work with a larger sample will be needed to confirm this result for clusters in general. Outside the cooling region it seems unlikely that this difference can be explained by the more efficient sputtering of dust grains in cooling-flow clusters, since the densities of cooling-flow and non–cooling-flow clusters are similar in this region. The mixing of low-metallicity gas during a merger may be responsible for this difference.

We thank the anonymous referee for many useful suggestions and comments. We thank C. Metzler for making his theoretical abundance profiles available to us. We also thank J. Mohr for kindly providing us his *ROSAT* PSPC density profiles. J. A. I. thanks R. Dupke and G. Evrard for many useful comments and conversations. This research has made use of data obtained through the *BeppoSAX* Science Data Center and the High Energy Astrophysics Science Archive Research Center Online Service, provided by the NASA/Goddard Space Flight Center. This work has been supported by *Chandra* Fellowship grant PF 9-10009, awarded through the *Chandra* Science Center. The *Chandra* Science Center is operated by the Smithsonian Astrophysical Observatory for NASA under contract NAS 8-39073.

REFERENCES

Allen, S. W., & Fabian, A. C. 1998, MNRAS, 297, L63
Anders, E., & Grevesse, N. 1989, Geochim. Cosmochim. Acta, 53, 197
Boella, G., et al. 1997, A&AS, 122, 327
D'Acri, F., De Grandi, S., & Molendi, S. 1998, in The Active X-ray Sky: Results from *BeppoSAX* and RXTE, ed. L. Scarsi, H. Bradt, P. Giommi, & F. Fiore (Amsterdam: Elsevier), 581
De Grandi, S., & Molendi, S. 1999a, A&A, 351, L45
———. 1999b, ApJ, 527, L25
Draine, B. T., & Salpeter, E. E. 1979, ApJ, 231, 77
Dupke, R. A., & White, R. E., III. 2000a, ApJ, 528, 139
———. 2000b, ApJ, 537, 123
Ettori, S., & Fabian A. C. 1999, MNRAS, 305, 834
Evrard, A. E., Metzler, C. A., & Navarro, J. F. 1996, ApJ, 469, 494
Ezawa, H., Fukazawa, Y., Makishima, K., Ohashi, T., Takahara, F., Xu, H., & Yamasaki, N. Y. 1997, ApJ, 490, L33
Fabian, A. C., Crawford, C. S., Edge, A. C., & Mushotzky, R. F. 1994, MNRAS, 267, 779
Finoguenov, A., David, L. P., & Ponman T. J. 2000, ApJ, 544, 188

Fujita, Y., Koyama, K., Tsuru, T., & Matsumoto, H. 1996, PASJ, 48, 191
Fukazawa, Y., Makishima, K., Tamura, T., Ezawa, H., Xu, H., Ikebe, Y., Kikuchi, K., & Ohashi, T. 1998, PASJ, 50, 187
Gaetz, T. J., Salpeter, E. E., & Shaviv, G. 1987, ApJ, 316, 530
Gunn, J. E., & Gott, J. R. 1972, ApJ, 176, 1
Henry, J. P., & Briel, U. G. 1996, ApJ, 472, 137
Ikebe, Y., et al. 1997, ApJ, 481, 660
Irwin, J. A., & Bregman, J. N. 2000, ApJ, 538, 543
Ishimaru, Y., & Arimoto, N. 1997, PASJ, 49, 1
Kaastra, J. S., Bleeker, J. A. M., & Mewe, R. 1998, in The Active X-ray Sky: Results from *BeppoSAX* and RXTE, ed. L. Scarsi, H. Bradt, P. Giommi, & F. Fiore (Amsterdam: Elsevier), 567
Kikuchi, K., Furusho, T., Ezawa, H., Yamasaki, N., Ohashi, T., Fukazawa, Y., & Ikebe, Y. 1999, PASJ, 51, 301
Metzler, C. A., & Evrard, A. E. 1994, ApJ, 437, 564
———. 1997, unpublished
Mohr, J. J., Mathiesen, B., & Evrard, A. E. 1999, ApJ, 517, 627
Molendi, S. 1998, *BeppoSAX* Technical Report
Molendi, S., & De Grandi, S. 1999, A&A, 351, L41
Molendi, S., De Grandi, S., & Fusco-Femiano, R. 2000, ApJ, 534, L43
Molendi, S., De Grandi, S., Fusco-Femiano, R., Colafrancesco, S., Fiore, F., Nesci, R., & Tamburelli, F. 1999, ApJ, 525, L73
Oegerle, W. R., & Hill, J. M. 1994, AJ, 107, 857
Oegerle, W. R., Hill, J. M., & Fitchett M. J. 1995, AJ, 110, 32
Ostriker, A., & Yahil, J. P. 1973, ApJ, 185, 787
Peres, C. B., Fabian, A. C., Edge, A. C., Allen, S. W., Johnstone, R. M., & White, D. A. 1998, MNRAS, 298, 416
Sarazin, C. L., Wise, M. W., & Markevitch, M. L. 1998, ApJ, 498, 606
Takahashi, T., Markevitch, M., Fukazawa, Y., Ikebe, Y., Ishisaki, Y., Kikuchi, K., Makishima, K., & Tawara, Y. 1995, *ASCA* Newsletter, 3 (NASA/GSFC)
Tamura, T., et al. 1996, PASJ, 48, 671
Watanabe, M., Yamashita, K., Kunieda, H., & Tawara, Y. 1997, in X-ray Imaging and Spectroscopy of Cosmic Hot Plasmas, ed. F. Makino & K. Mitsuda (Tokyo: Universal Academy), 131
White, D. A. 2000, MNRAS, 312, 663
White, D. A., Jones, C., & Forman, W. 1997, MNRAS, 292, 419